Denisov M.S., Finikov D.B.

Amplitude spectrum estimation method and «amplitude deconvolution» method.

Wavelet amplitude spectrum estimation is one of the problems dealt with in different applications of digital signal processing. This is also a well - known problem in seismic exploration. Much research is devoted to its solution. Many techniques developed for geophysical data processing have found practical use in quite different fields (for example, Burg's maximum entropy spectrum estimation), but they proved to be not effective in seismic exploration. It is due to some specific features of seismic traces which will be briefly discussed below. A new spectrum estimation method and a corresponding spectrum balancing technique ("amplitude deconvolution") are presented in this paper. Though this method is based on several well - known and practically useful principles, it has the following advantage over the conventional methods: it makes it possible to take into account some important characteristics of seismic traces.

The problem is formulated in the traditional manner: the seismic trace $z(t)$ is considered in terms of the convolutional model $y(t) = s(t) * \xi(t)$ with additive noise $n(t)$, i.e.

$$z(t) = y(t) + n(t) = s(t) * \xi(t) + n(t), \qquad (1)$$

where t is the discrete time, $s(t)$ - the wavelet, $\xi(t)$ - the reflectivity response, $n(t)$ - noise, uncorrelated with $y(t)$. The wavelet $s(t)$ may consist of several convolutional terms.

The reflectivity $\xi(t)$ is considered to be stationary white noise, i.e.

$$M\{\xi(t)\xi(t+\tau)\} = \sigma^2\delta(\tau).$$

All the spectrum estimation and deconvolution problem solutions concern the problem of either the wavelet $s(t)$ or its amplitude spectrum $|s(\omega)|$ estimation, where $s(\omega)$ is the Fourier transformation of $s(t)$.

The power spectrum of time series (1) obeys the equation

$$P(\omega) = \sigma^2|s(\omega)|^2 + |n(\omega)|^2, \qquad (2)$$

where $|n(\omega)|^2$ is the power spectrum of the noise.

Here the spectrum estimation problem is treated as the $P(\omega)$ estimation problem. It may be important to estimate $|s(\omega)|$ and $|n(\omega)|$ separately, but such a problem is not considered in this paper.

Many difficulties that the seismic trace spectrum estimation encounters are caused by $\xi(t)$ non - Gaussinity that manifests itself as the well - known "effect of the reflectivity response" on the power spectrum estimates. False spectrum splitting and the presence of spectrum outliers that cannot be smoothed are usually caused by this effect. Either taking into account the

statistical characteristics of $\xi(t)$, or utilising some a priori information about the sought-for power spectrum can be used to overcome it. The first way application causes the necessity of the wavelet phase spectrum estimation[1)] (this is a rather complicated problem that should be solved separately from the amplitude spectrum estimation problem.

The paper is devoted to the development of the wavelet amplitude spectrum estimation and deconvolution techniques that require the most general a priori information about the seismic trace power spectrum.

Let us consider the noise-free problem at first. Suppose that

$$|s(\omega)| = \alpha_0 \exp[\sum_{i=1}^{N} \alpha_i \psi_i(\omega)], \qquad (3)$$

$$\psi_i(\omega) = \cos[i \frac{(\omega - \omega_1)}{\omega_2 - \omega_1}]. \qquad (3')$$

for $\omega \in (\omega_1, \omega_2)$. Nearly all the possible amplitude spectra can be approximated by this decomposition (Korn, G.A., Korn, T.M., 1968). The constraint imposed on N, the number of the wavelet logarithmic amplitude spectrum decomposition terms (it must not be too large), implies its smoothness, i.e. the amplitude spectrum should not contain outliers. Thus, this limitation narrows the area of possible solutions.

Another important constraint on the wavelet amplitude spectrum decomposition parameters is introduced

$$\sum_{i=1}^{N} (\alpha_i)^2 \le \hat{\rho}. \qquad (4)$$

This constraint will be discussed later, but even now it is clear that only smooth $|s(\omega)|$ can be approximated by (3) taking into account (4).

Let

$$\overline{\psi}_i(\omega) = \begin{cases} \psi_i(\omega), \omega \in (\omega_1, \omega_2) \\ 0, \omega \notin (\omega_1, \omega_2) \end{cases} \qquad (5)$$

and let $f(t, \tilde{\alpha})$ be the filter that has the following amplitude spectrum:

$$|f(\omega, \tilde{\alpha})| = \exp[\sum_{i=1}^{N} \tilde{\alpha}_i \overline{\psi}_i(\omega)]. \qquad (6)$$

We have to estimate $\hat{\alpha} = \{\hat{\alpha}_1, \hat{\alpha}_2, ..., \hat{\alpha}_N\}$ that minimises the objective

$$J_{\hat{\rho}}(\tilde{\alpha}) = \sum_{t=T_1}^{T_2} (f(t, \tilde{\alpha}) * z(t))^2 \qquad (7)$$

---

1) This is due to the dependence of the probability density function of the random process (1) upon the wavelet phase.

satisfying the constraint

$$\sum_{i=1}^{N} (\tilde{\alpha}_i i)^2 \le \hat{\rho}, \qquad (8)$$

where (T_1, T_2) is the spectrum estimation time gate.

It can be easily seen from (3) - (8) that the amplitude spectrum estimation problem statement, the constraint and the spectrum decomposition technique are similar to those used for the phase deconvolution problem solution presented in the previous report. But in fact they differ significantly. The objective (7) has the same sense as the well - known and widely used in spectrum estimation problem solutions prediction error dispersion. This is valid due to the choice of the least squares objective, i.e. the objective remains the same for the filter $f(t, \tilde{\alpha})$ having an arbitrary phase. For example, $f(t, \tilde{\alpha})$ can be minimum - phase. Its logarithmic amplitude spectrum and phase form a Hilbert transform pair. To obtain this phase for a broadband case $(\omega_1 = 0, \omega_2 = \pi)$ *cos* should be replaced by *sin* in (3′). Then (3) will be the phase. It is easy to see[2)] that such a minimum - phase filter has its first sample equal to 1, hence, it is similar to the prediction error operator, i.e. it is $(1, f(1, \tilde{\alpha}), f(2, \tilde{\alpha}), \ldots)$. So, having minimised the objective (7) with respect to $\tilde{\alpha}$, we obtain the optimal prediction error operator.

The filter obtained differs from the conventional prediction error filter because its amplitude spectrum is presented by the decomposition (6) taking into account the constraint (8). This fact implies that if the wavelet amplitude spectrum can be represented by decomposition (6) we shall obtain its estimate that has the same properties as the prediction error based estimate, e.g. this estimate will be consistent.

In the presence of additive noise $n(t)$ the power spectrum (2) will be estimated.

The proposed way of amplitude spectrum decomposition is similar to the cepstrum one. The differences lie in the possibility of the limited spectrum band (ω_1, ω_2) decomposition and in the application of the optimisation procedure to estimate the sought-for parameters. But the algorithm has got all the advantages of cepstral methods.

Decomposition within a limited band makes us able to get rid of the difficulties that are faced while using the predictive deconvolution algorithm or any other algorithm of parametric spectrum estimation. Overcoming these difficulties requires application of data resampling in time domain (or spectrum

---

[2)] This is due to the following property of the decomposition used: $\int_0^{\pi} \sum_{i=1}^{N} \tilde{\alpha}_i \varphi_i(\omega) = 0$ for any $\tilde{\alpha}$.

transformation from $[0,\pi)$ into (ω_1,ω_2) band in frequency domain) used in the selective deconvolution algorithm (Malkin, A., Sorin, A., and Finikov, D., 1985, Selective spiking deconvolution of seismic traces: Oil and gas geology, geophysics and drilling, N. 10. (in Russian)).

Parameter $\hat{\rho}$ (see (8)) turns out to be a very important one. To introduce a constraint on the parameters $\tilde{\alpha}$ obtained, the "complexity" of the corresponding prediction error operator is measured. Varakin, L.,1970, (Theory of complex signals: Soviet radio. (in Russian)) showed that the "complexity" of the wavelet is determined mainly by its phase spectrum. Hence, it seems useful to limit the length of a phase filter[3)] after its resampling or spectrum transformation into (ω_1,ω_2) band. The "complexity" of a broadband wavelet $w(t)$ can be treated as its length

$$l = \frac{\sum_{t=-\infty}^{\infty}(w(t)t)^2}{\sum_{t=-\infty}^{\infty}(w(t))^2}.$$

It can be proved that for a phase filter $l = \tilde{\rho} = \sum_{i=1}^{N}(\tilde{\alpha}_i i)^2$. Since the logarithmic amplitude spectrum of a minimum - phase filter and its phase form a Hilbert transform pair, the presence of distortions of the amplitude spectrum estimate caused by the "effect of the reflectivity response" leads to the presence of its phase distortions. That is why the shape of this filter and its "complexity" depend on the "effect of the reflectivity response".

Let us consider an example. The synthetic reflectivity and the synthetic trace are given in Figure 1. The wavelet amplitude spectrum is presented by the decomposition (3) with $N = 7$ and $\alpha = \{-0.20,-0.10,0.10,0.20,-0.20,0.20,-0.05\}$. The length of the phase filter: $\tilde{\rho} = 1.85$. This phase filter and the prediction error filter are also presented in Figure 1.

[3)] ***phase filter*** is a broadband wavelet that has a flat amplitude spectrum and the phase spectrum given by decomposition (3), (3′) after replacing $\cos$ by $\sin$.

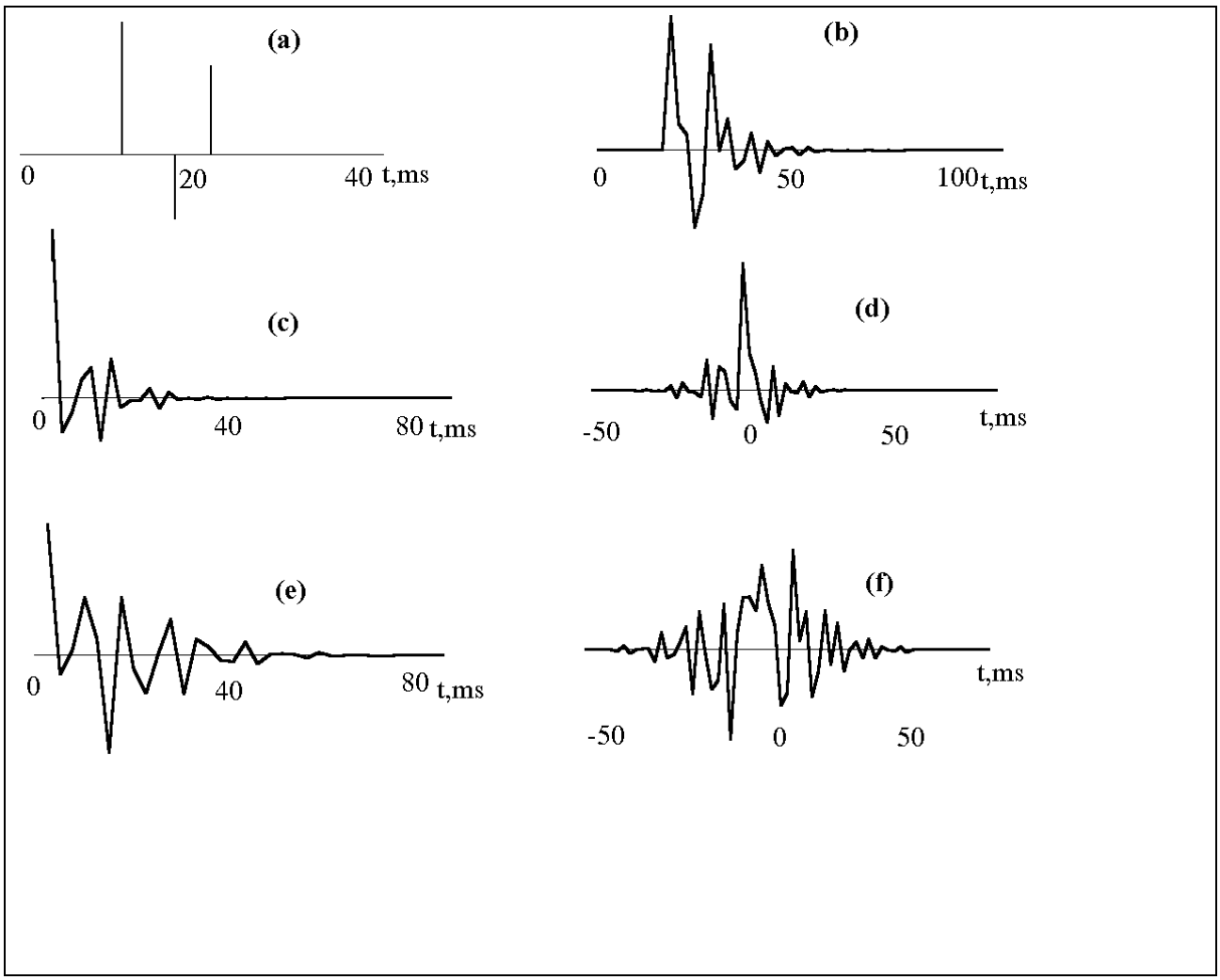

Figure 1. The results of testing of the "effect of the reflectivity response" on the "complexity" of the prediction error filter. (a) Reflectivity, (b) synthetic trace, (c) and (d) prediction error filter and phase filter respectively that were computed from the wavelet, (e) and (f) prediction error filter and phase filter respectively that were computed from the synthetic trace.

The objective (7) computed from the synthetic trace without constraint (8) has minimum at the point $\tilde{\alpha} = \{-0.14, 0.03, 0.45, 0.20, -0.73, 0.22, 0.12\}$. $\tilde{\rho}$ is equal to 4.3. The prediction error filter obtained and the corresponding phase filter are shown in Figure 1. It is evident that the prediction error filter obtained is more "complex" that the sought-for one.

It can be proved that the objective (7) has only one minimum, hence it is easy to find it.

If the constraint (8) is introduced it will be useful to apply the following two step algorithm:

1) minimise the objective without (8), find the solution and the corresponding parameter $\tilde{\rho}$;

2) introduce (8) and adjust the solution obtained at the first step. To do this some $\Delta\rho$ should be specified and the iterative procedure should be started. At

step k of this procedure the parameter $\tilde{\rho}^k$ should be obtained as $\tilde{\rho}^k = \tilde{\rho}^{k-1} - \Delta\rho$ and the sought-for vector $\hat{\alpha}^k$ should be estimated (i.e. a projection of the solution $\hat{\alpha}^{k-1}$ on the ellipsoid given by (8) should be carried out and after it the parameters $\hat{\alpha}^k$ should be obtained by minimising the objective (7) in the vicinity of this projection[4]).We proceed these iterations until $\tilde{\rho}^k \geq 0$ and then choose the parameter $\hat{\rho}$ that is equal to the least value of $\tilde{\rho}^k$ that does not significantly influence the prediction error dispersion. The plot of the objective $J_{\tilde{\rho}}(\hat{\alpha})$ as the function of $\tilde{\rho}$ is supposed to have maximum at the point $\tilde{\rho} = 0$,decrease rapidly for low $\tilde{\rho}$ and slightly decrease for $\tilde{\rho} \geq \rho^{wav}$, where $\rho^{wav} = \sum_{i=1}^{N} (\hat{\alpha}_i^{wav} i)^2$, $\hat{\alpha}^{wav}$ is the minimum of the objective (7) for $z(t) = s(t)$ without constraint (8). Such a shape of the plot is supposed to be conventional because balancing of distortions of the amplitude spectrum (they are caused by the "effect of the reflectivity response") cannot influence significantly such an integral parameter as the prediction error dispersion. On the other hand, as it was discussed earlier, balancing of the outliers can be effected only by a "complex" filter, i.e. this will result in $\tilde{\rho}$ increase. So, the following choice of the parameter $\hat{\rho} \leq \rho^{wav}$ is valid.

Inverse filtering of a trace by operator $f(t, \hat{\alpha})$, calculated as it was described above, will be called *amplitude deconvolution*.

An effective procedure that takes into account the specific features of this problem was developed to calculate the filter $f(t, \hat{\alpha})$.

The basic ideas of cepstral methods and spiking deconvolution (including the selective deconvolution) are combined and used by the new algorithm. Moreover, it can be said that the cepstrum methods are considered in terms of spiking deconvolution. But while the spiking deconvolution is based on the finite order autoregressive model of seismic trace and smoothness of the amplitude spectrum obtained is controlled by the order of the model (or by the length of the prediction operator, that is the same), the new algorithm uses an infinite order autoregression. Smoothness is controlled by setting the length $\hat{\rho}$ of the phase filter. The complexity of the model (3) is defined by its order N. So, it is possible to solve the problems of the model order determination and spectrum smoothing separately.

Let us consider the following synthetic example: a wavelet

---

[4] It is important to stress that though the objective (7) without (8) is unimodal, it is not unimodal at the ellipsoid given by (8). Nevertheless it is easy to obtain the desired minimum because the projection of the previous solution is used as the starting point for the search.

$$s(t) = \begin{cases} (0.9)^t \cos(50\pi t), t > 0 \\ (0.7)^{-t} \cos(100\pi t), t < 0 \end{cases},$$

and its amplitude spectrum (it can be precisely presented by decomposition (3) only for $N \to \infty$) are shown in Figure 2. Synthetic traces with and without additive noise and the periodogram are also presented in Figure 2. This is a complicated test for spectrum estimation for the gate is small, the wavelets interfere not so severely as to enable the spiking deconvolution provide good spectrum estimates (this algorithm is effective for Gaussian processes).

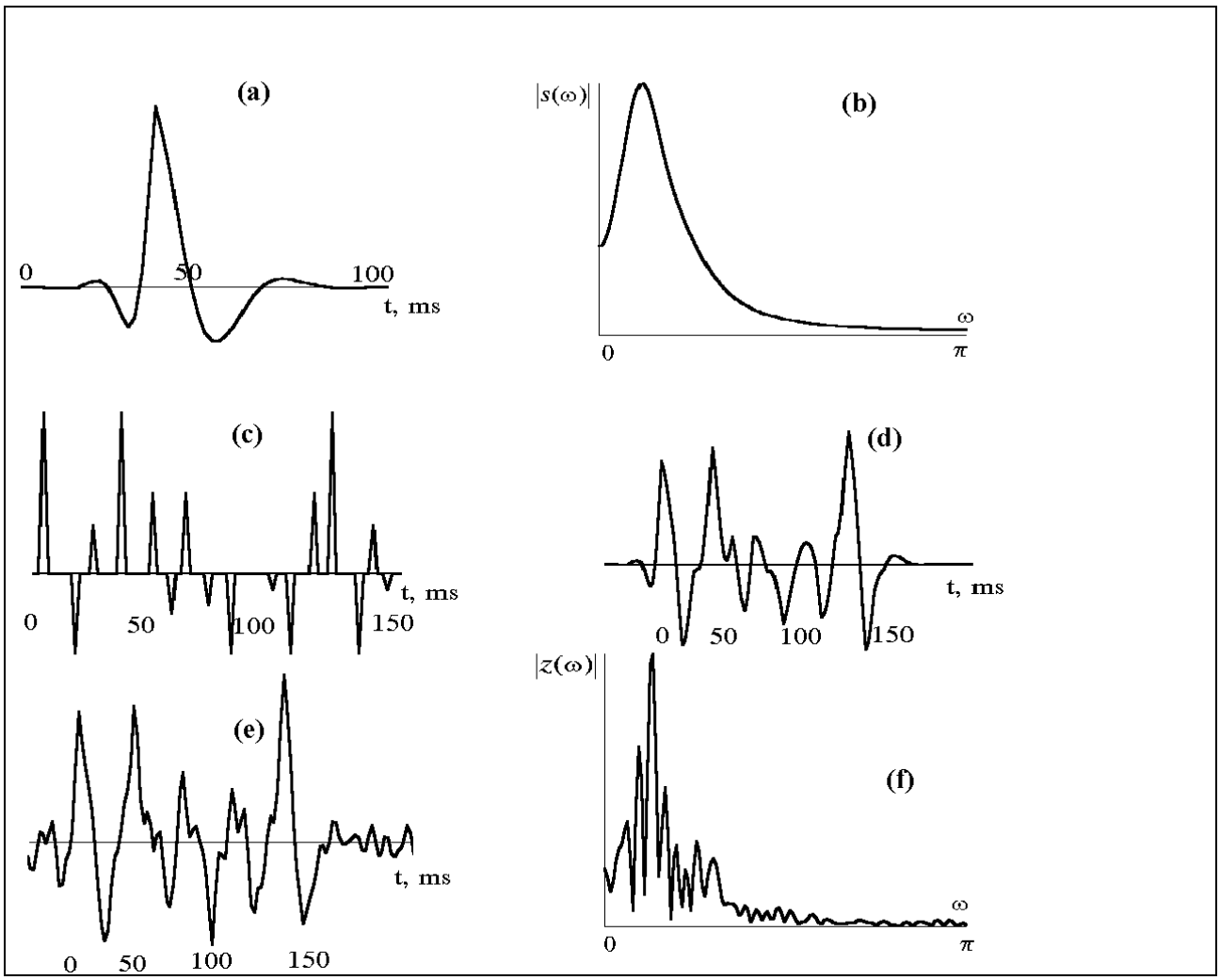

Figure 2. (a) Synthetic wavelet, (b) its amplitude spectrum, (c) reflectivity, (d) noise - free synthetic trace, (e) noisy synthetic trace, (f) periodogram of the noise - free trace.

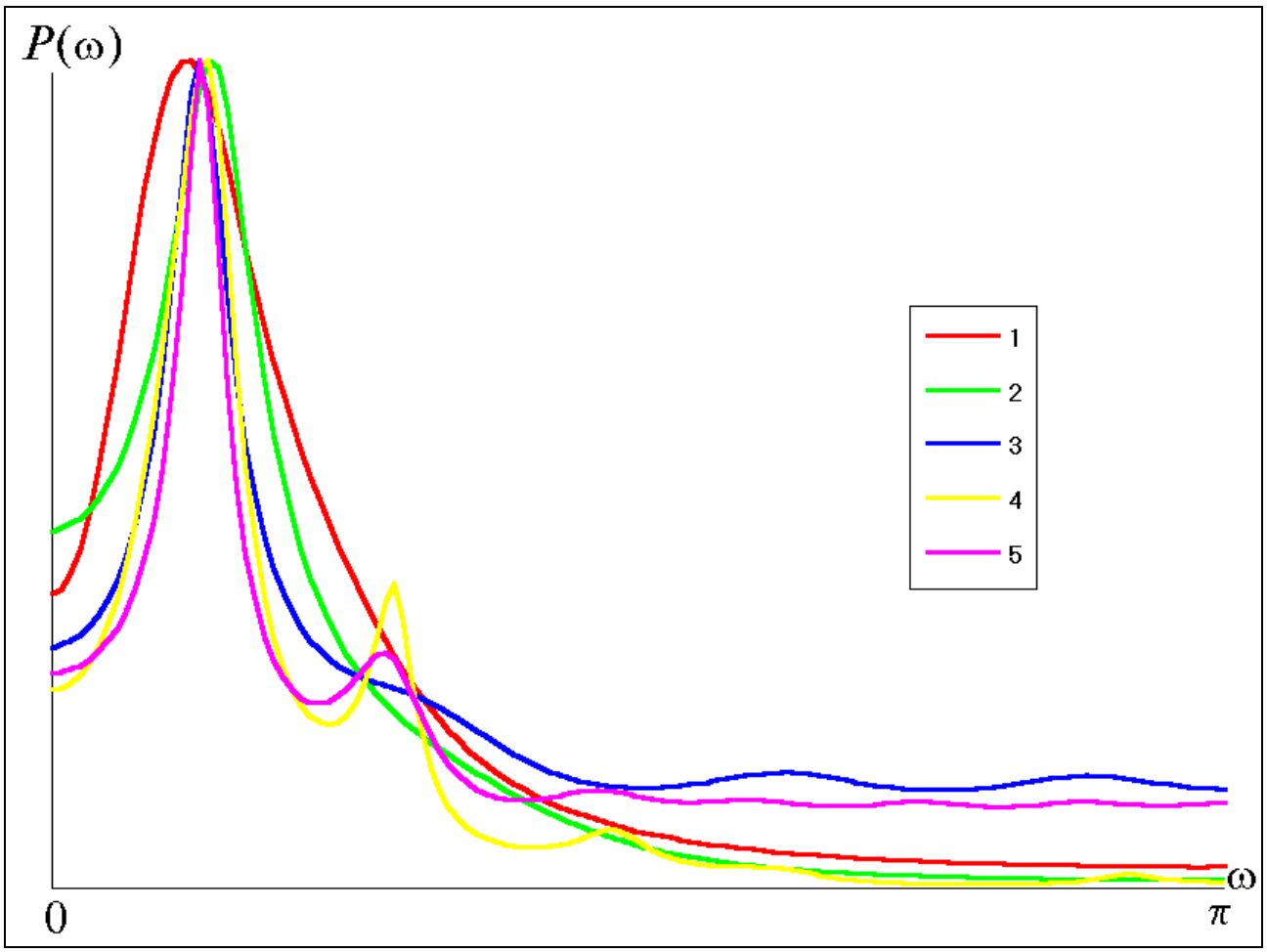

Figure 3. Amplitude spectrum estimates via spiking deconvolution. (1) The wavelet's amplitude spectrum. (2), (3), (4) and (5) - spectra obtained by application of 4, 8, 12 and 15 - point prediction operators respectively.

Four spiking deconvolution spectrum estimates are presented in Figure 3. They are obtained from the noise - free trace for different lengths of predictors. Note that increase of the filter length makes the estimate look like the periodogram and its decrease causes smoothness of the estimates, but they have nothing to do with the desired amplitude spectrum. This example clearly demonstrates the drawbacks of the spiking deconvolution as well as the drawbacks of any parametric spectrum estimation algorithm.

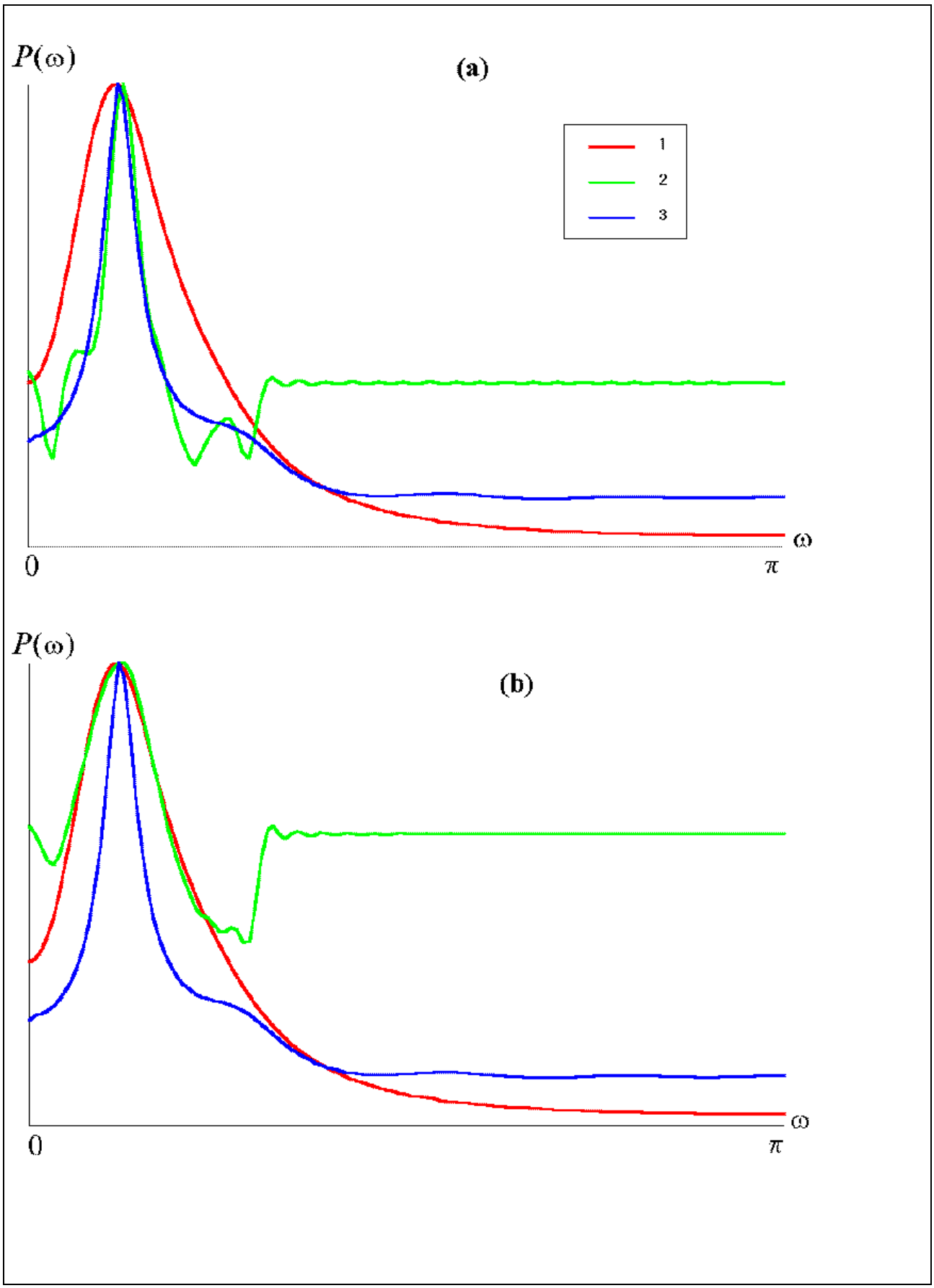

Figure 4. Spectrum estimates obtained from the noise - free trace. (1) The wavelet's amplitude spectrum, (2) the new algorithm application result, (3)

spiking deconvolution estimate (N - point prediction operator). (a) One - step procedure result, (b) two - step procedure result.

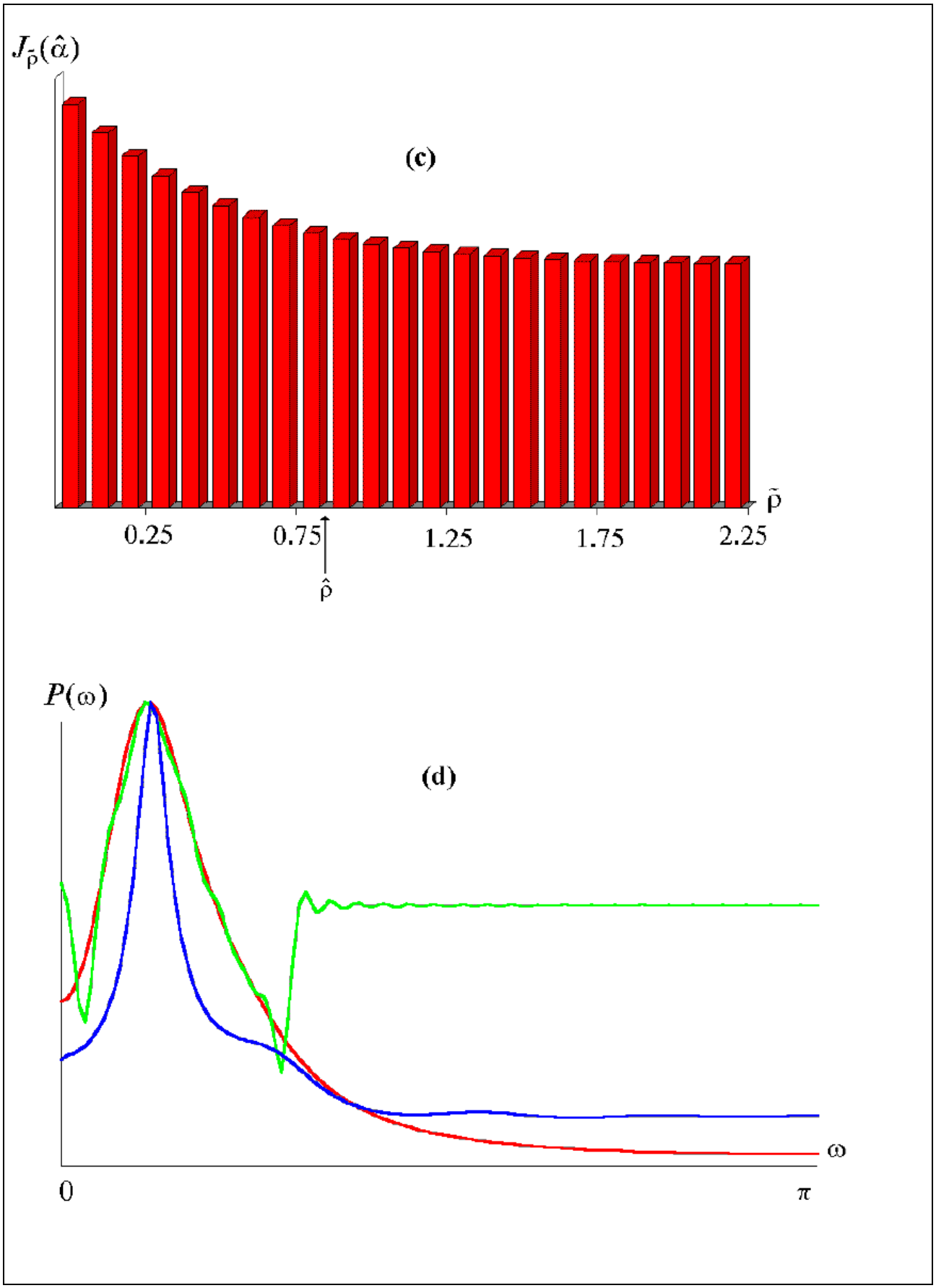

Figure 4. (c) the plot of the objective $J_{\tilde{\rho}}(\hat{\alpha})$ as the function of $\tilde{\rho}$, (d) spectrum estimate calculated from the wavelet itself ($z(t) = s(t)$).

A spectrum estimate provided by the new algorithm for $N = 10$ is given in Figure 4. A noise - free trace was chosen and the objective was minimised without the constraint (i.e. only the first step was applied). The values ω_1 and ω_2 were set $5Hz$ and $75Hz$ respectively, $\Delta t = 2ms$. This estimate is similar to the 10 - point spiking deconvolution estimate and it has distortions similar to those of the periodogram. The estimate obtained by application of the two - step procedure is also shown in Figure 4. The plot of the objective $J_{\tilde{\rho}}(\hat{\alpha})$ as the function of $\tilde{\rho}$ is presented. As it was expected, it decreases rapidly for low values of $\tilde{\rho}$ and then it flattens. The value $\hat{\rho} = 0.80$ was chosen (it is noted by the arrow).

The results of spectrum estimation for $z(t) = s(t)$ are presented in Figure 4. The value $\rho^{wav} = 1.26$ was obtained. The estimated amplitude spectrum is smooth and it is close to the true spectrum within the band (ω_1, ω_2).

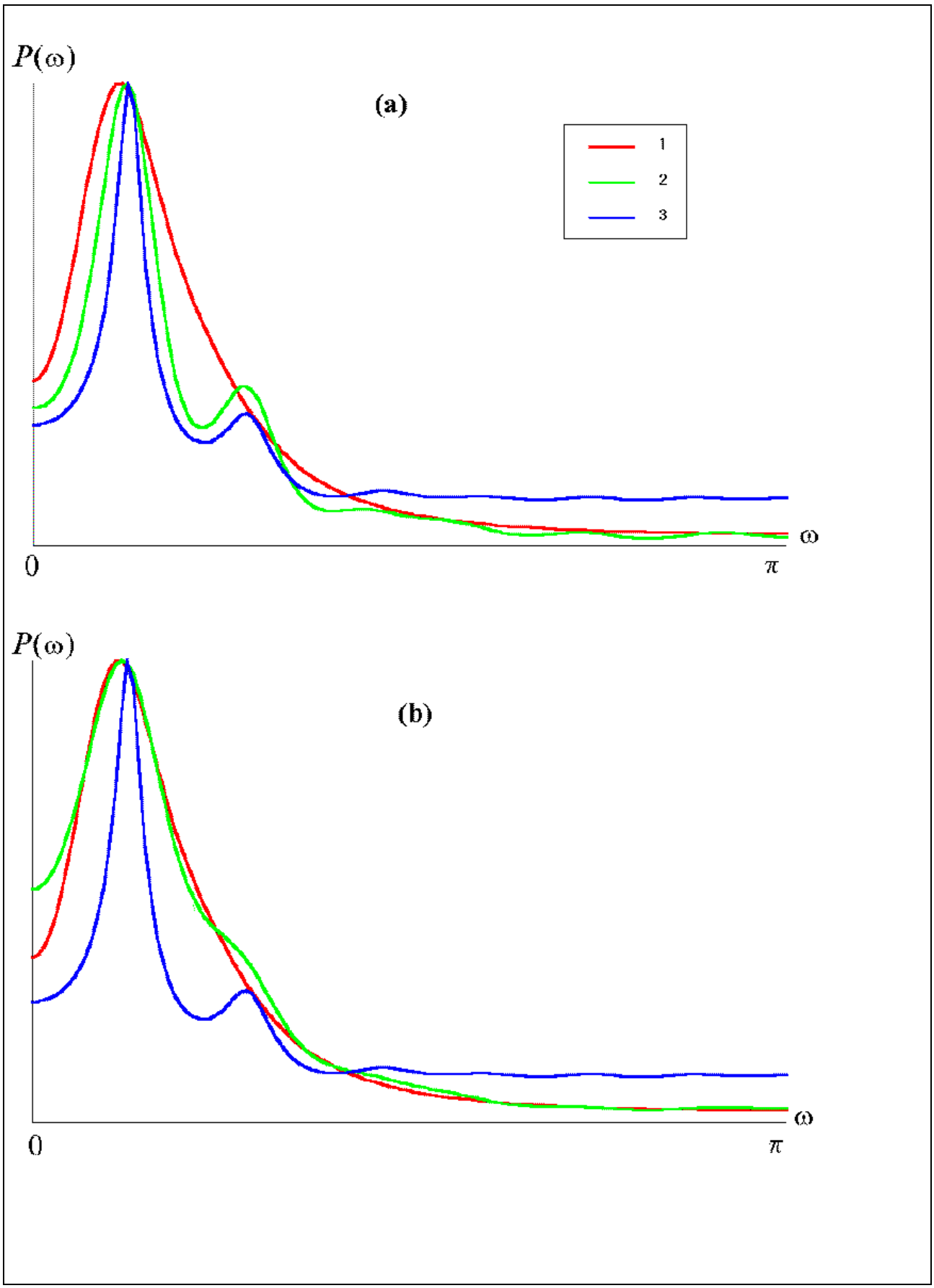

Figure 5. Broadband spectrum estimates obtained from the noise - free trace. (1) The wavelet's amplitude spectrum, (2) the new algorithm application result, (3)

spiking deconvolution estimate (N - point prediction operator). (a) One - step procedure result, (b) two - step procedure result.

It is clear that the narrower the band is, the less number of the basic functions is needed to approximate possible oscillations of amplitude spectrum. That is why it was set $N = 15$ for broadband tests. The results of calculations are given in Figure 5. The estimate obtained without constraint ($\tilde{\rho} = 4.30$) is not satisfactory. Introducing the constraint ($\hat{\rho} = 2.50$) results in the estimate improvement.

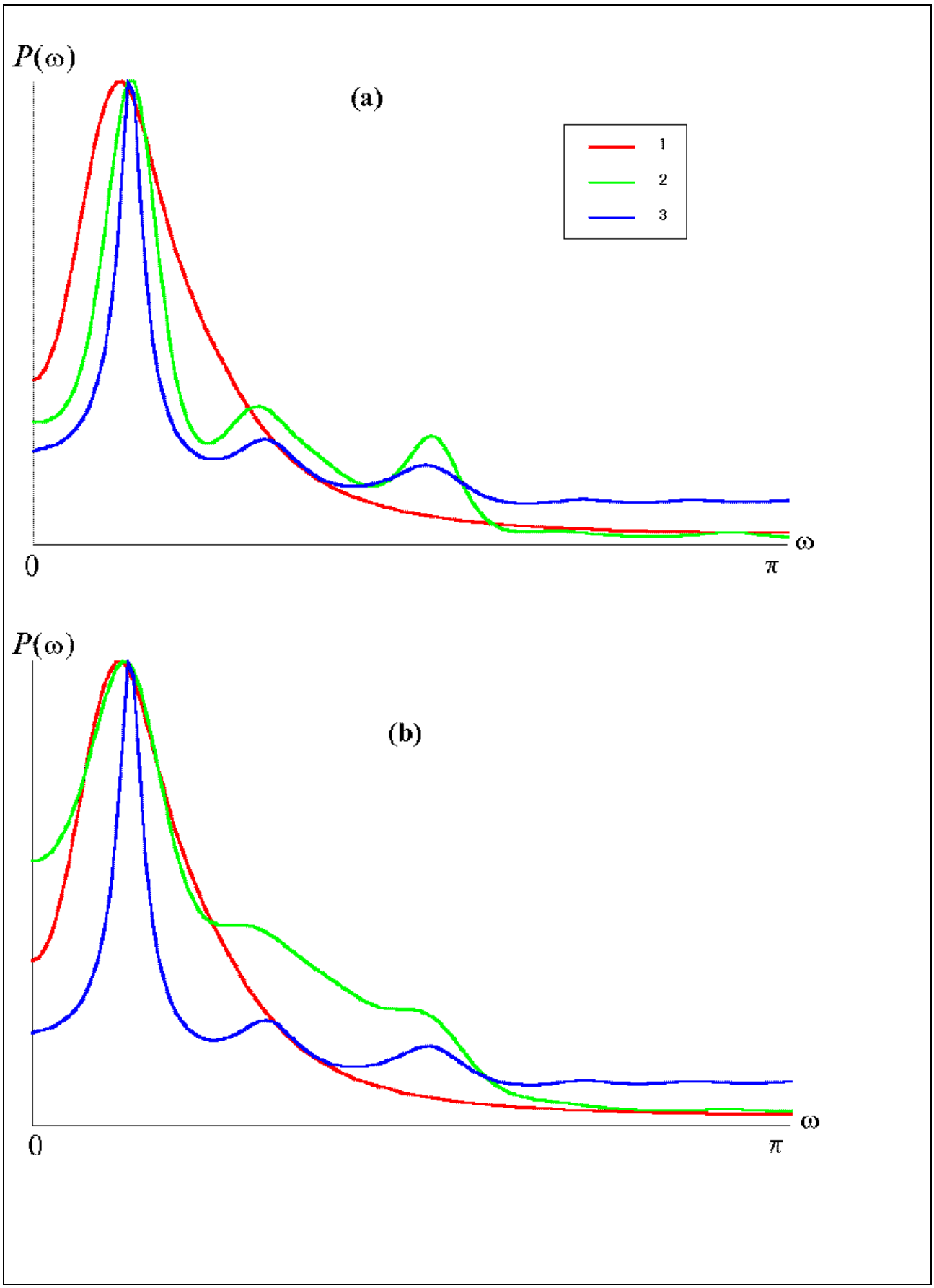

Figure 6. Broadband spectrum estimates obtained from the noisy trace. (1) The wavelet's amplitude spectrum, (2) the new algorithm application result, (3)

spiking deconvolution estimate (N - point prediction operator). (a) One - step procedure result, (b) two - step procedure result.

One - step ($\tilde{\rho} = 4.50$) and two - step ($\hat{\rho} = 2.50$) spectrum estimation results from a noisy trace are shown in Figure 6. It is clear that the estimate approximates the power spectrum $P(\omega)$ (see (2)) rather than the wavelet amplitude spectrum.

The following processing sequence is suggested for real data processing. After a filter adjusting gate is chosen on the section, the parameters of the filter ($\hat{\rho}$ and n) should be estimated. To do it, the curves like the one shown in Figure 4 (c) should be calculated. The parameters can be automatically calculated from these curves. Then the estimated parameters should be fixed for the whole line for its processing.

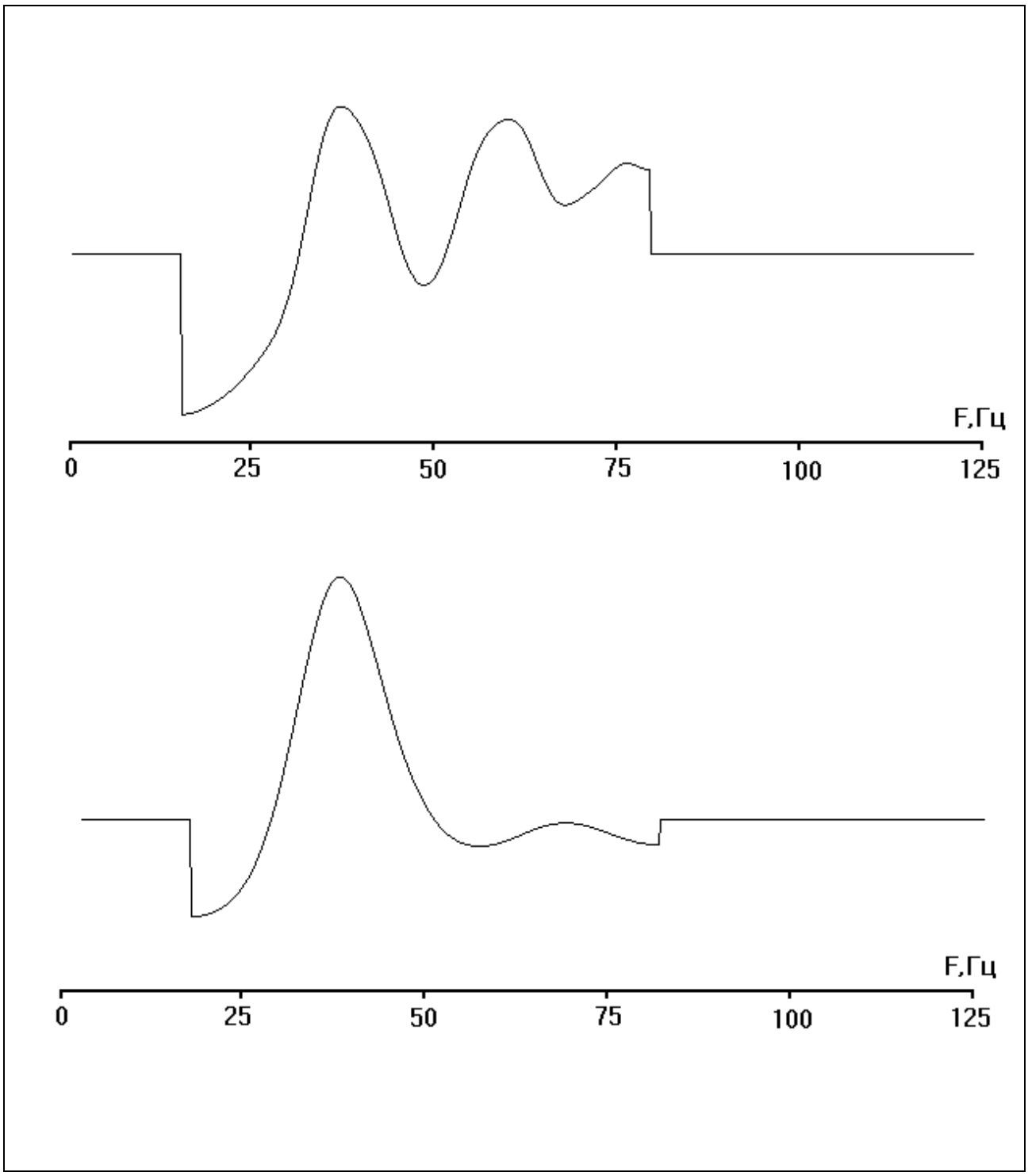

Figure 7. Power spectrum estimates within the band (15 - 80) Hz. (a) an estimate obtained from the shallow part of the stack, (b) an estimate obtained from the deeper part of the stack.

Let us consider a Western Siberia section as the real data example. The main problem one usually faces while processing these data is significant variation of the wavelet amplitude spectrum measured in the shallow part from the one in the deeper part due to absorption. Hence, only short time filter adjusting gates

can be set. An example of this amplitude spectrum variation is given in Figure 7.

It is important to point out that outside the band specified, the estimated spectrum is set constant of unit amplitude (see Figure 4, Figure 7). This way of treating the spectrum is implied by the basic idea of the algorithm, i.e. it balances amplitude spectrum within the band and preserves its shape outside it.

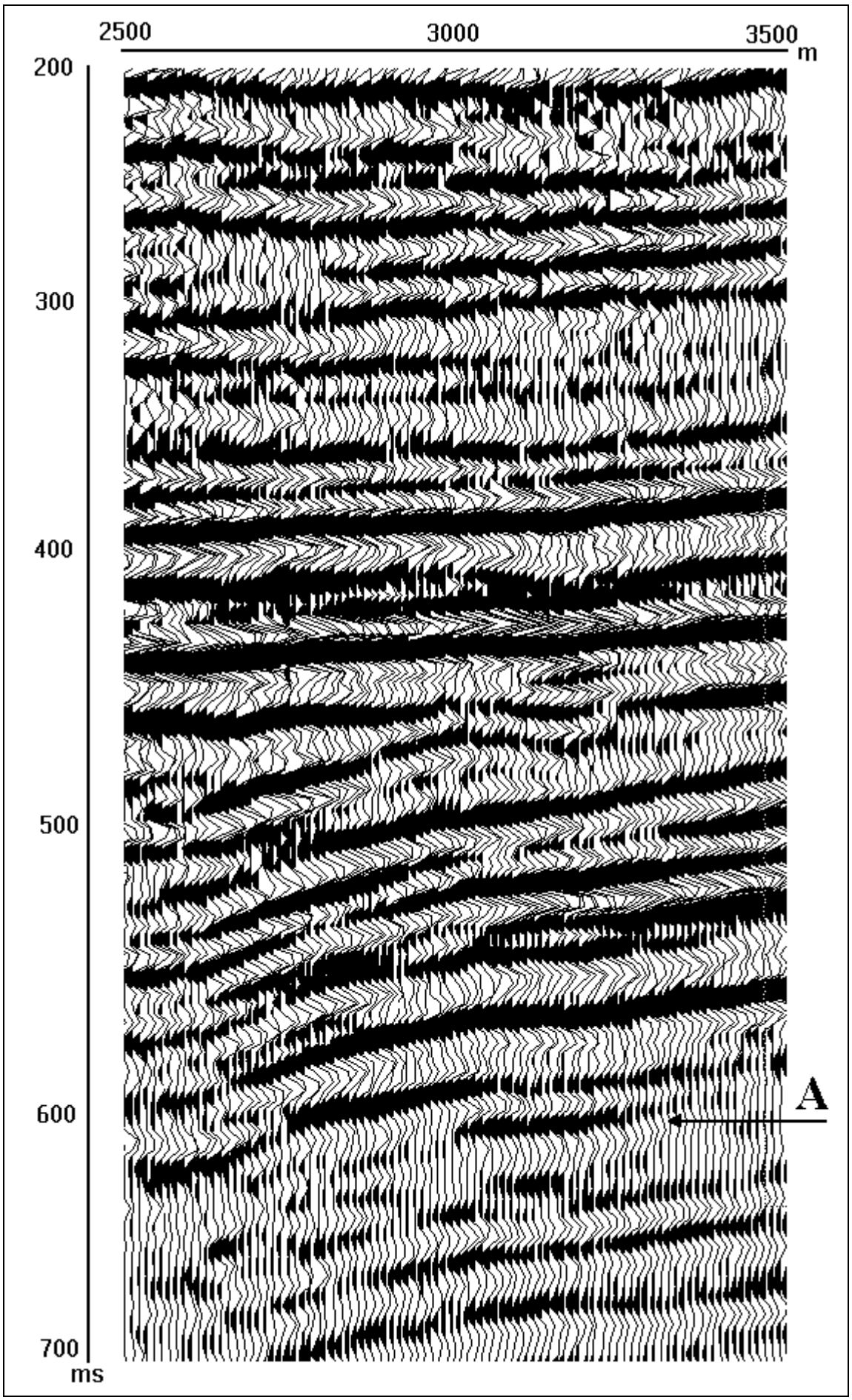
2500
3000
3500
m
200
300
400
500
600
700
ms
A

Figure 8(a). A Western Siberia stack shallow part processing results: a portion of the input stack.

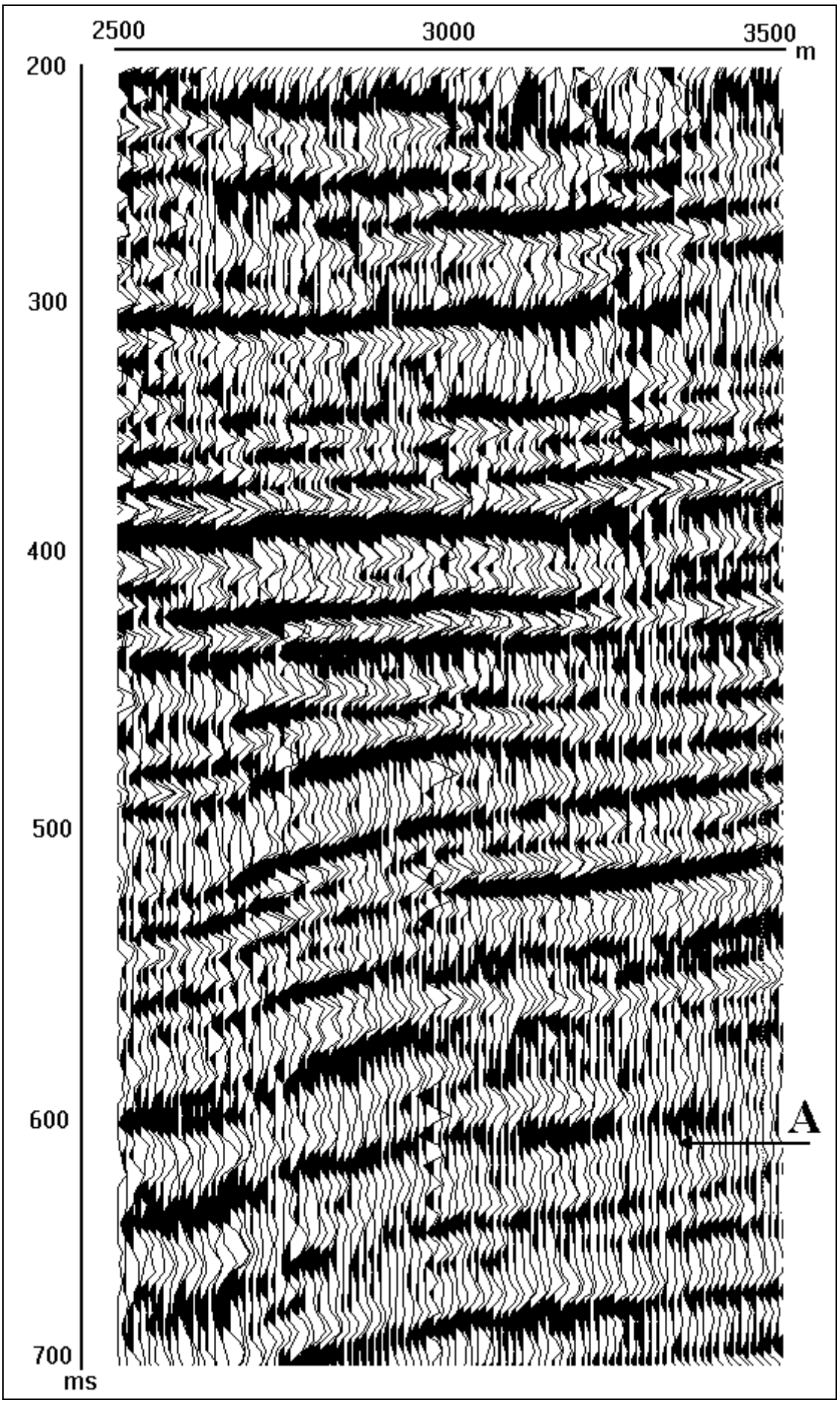

Figure 8(b). Spiking deconvolution.

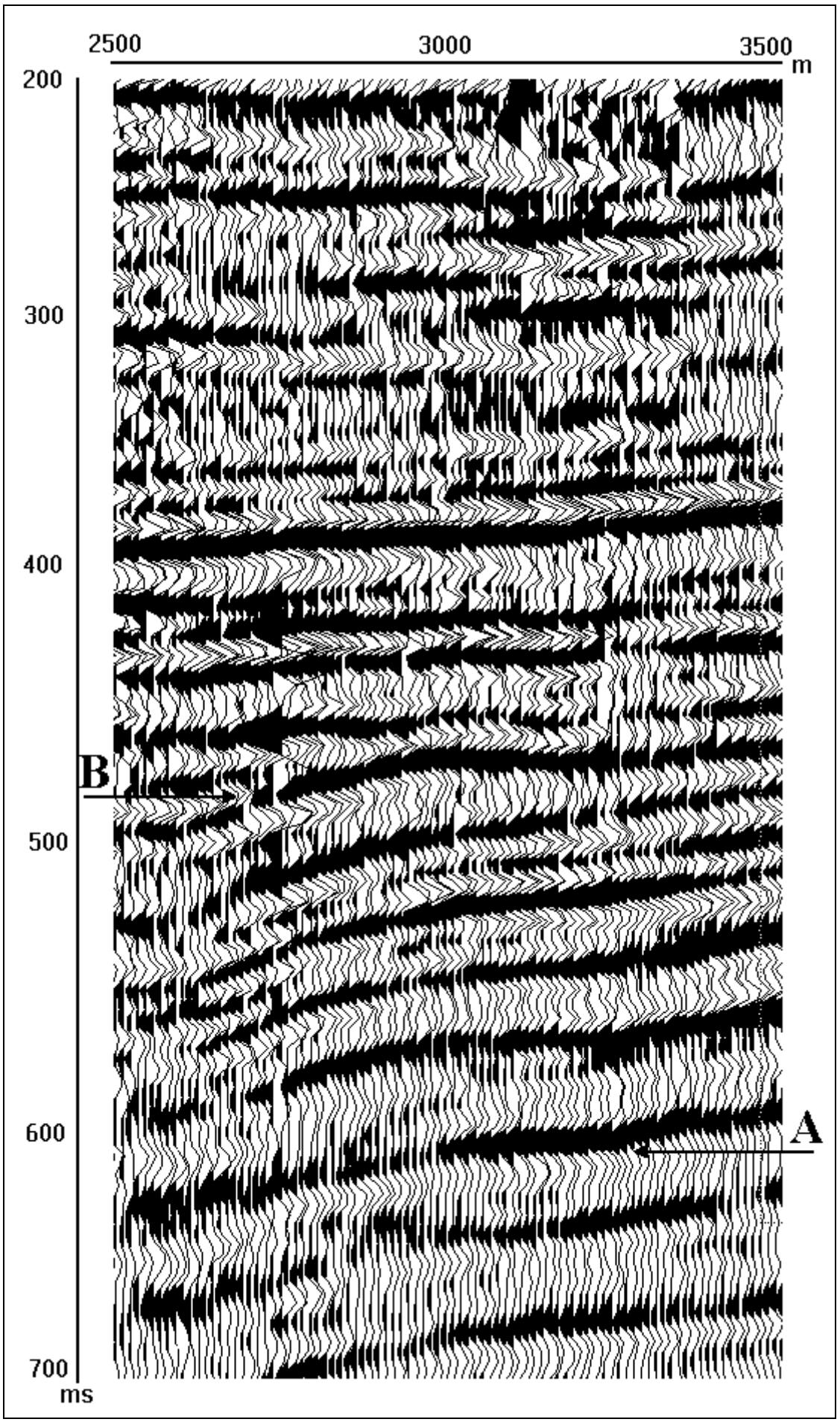

Figure 8(c). A constraint - free amplitude deconvolution.

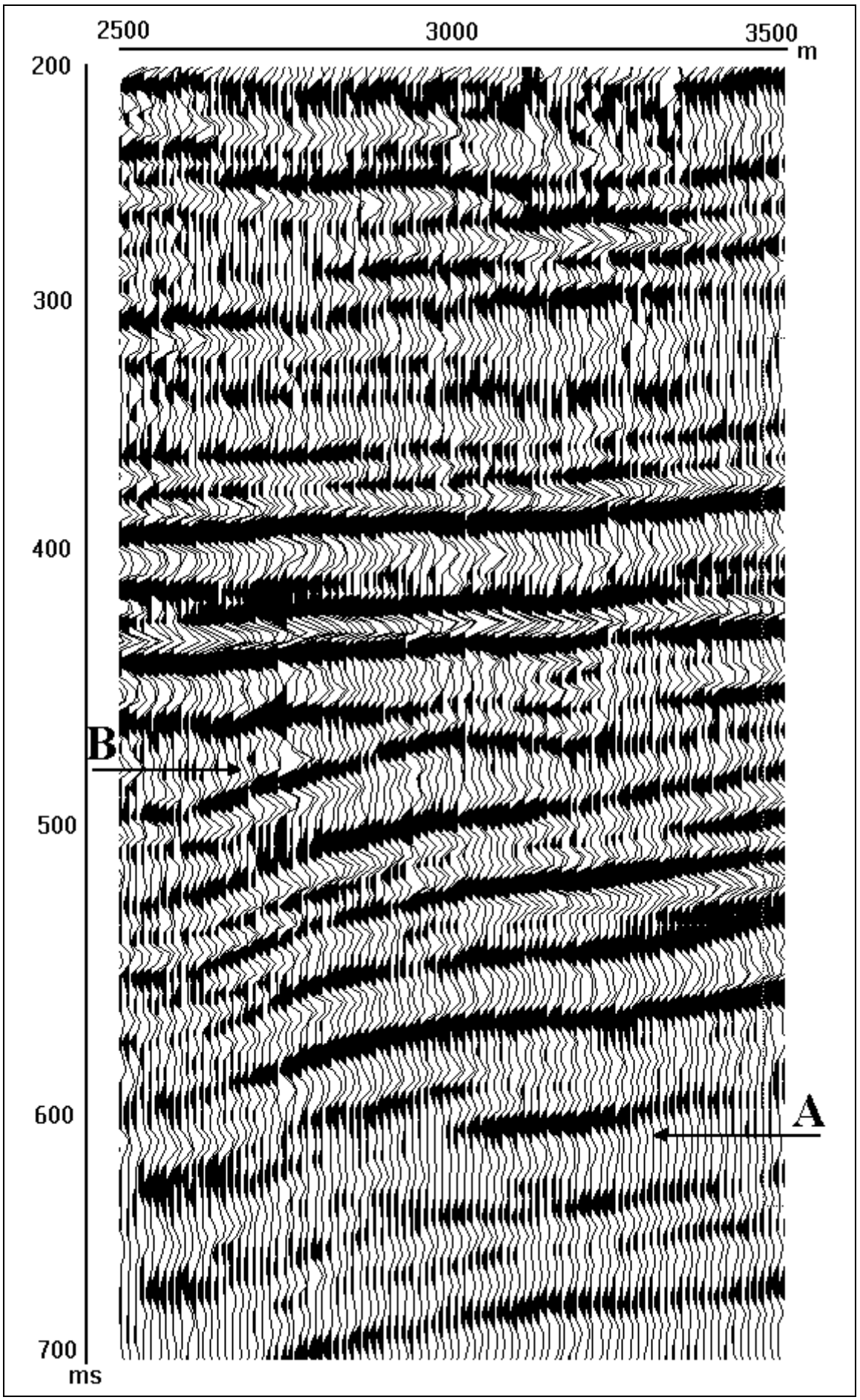

Figure 8(d). Amplitude deconvolution with constraint (8).

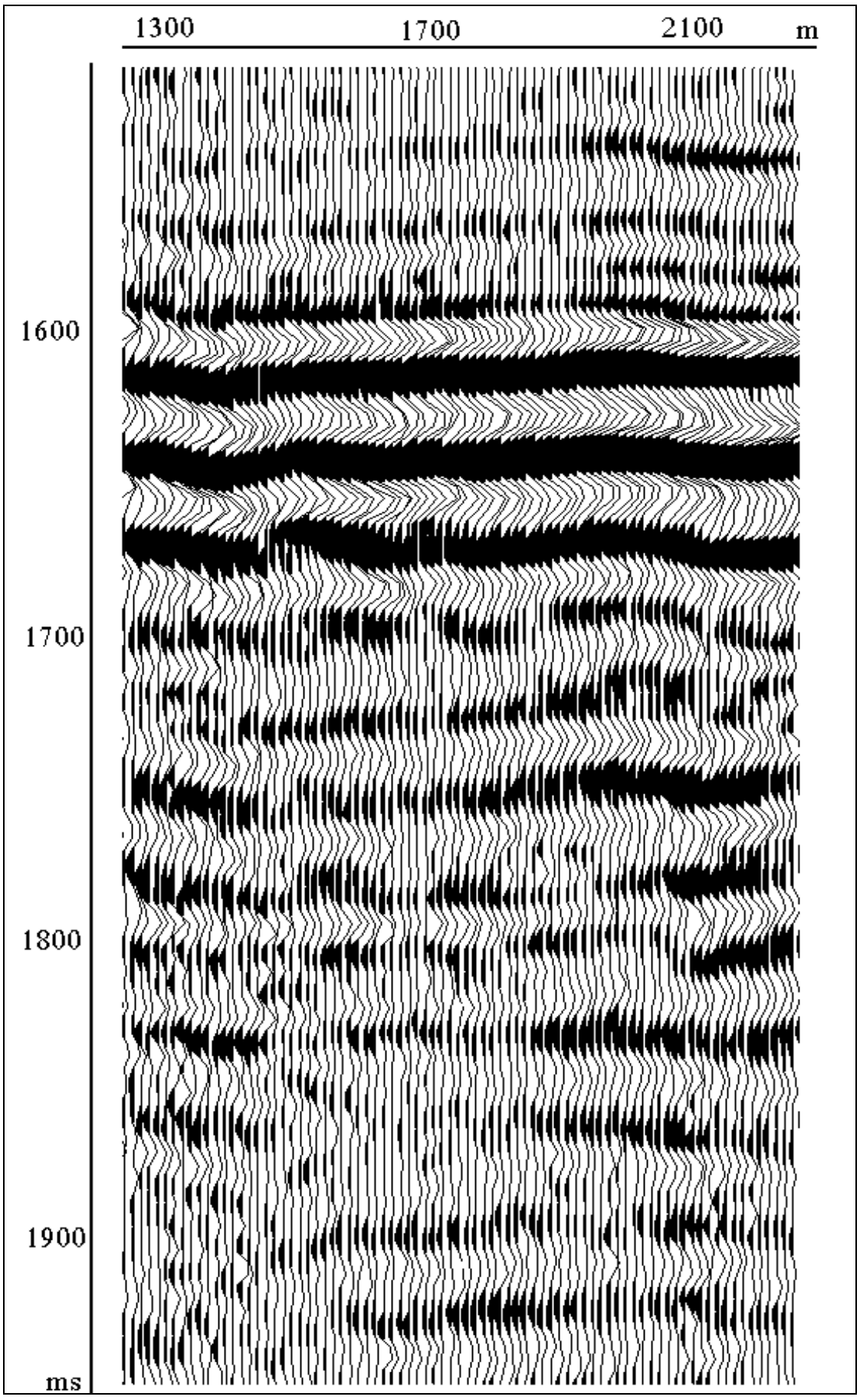

Figure 9(a). A Western Siberia stack deeper part processing results. A portion of the input stack

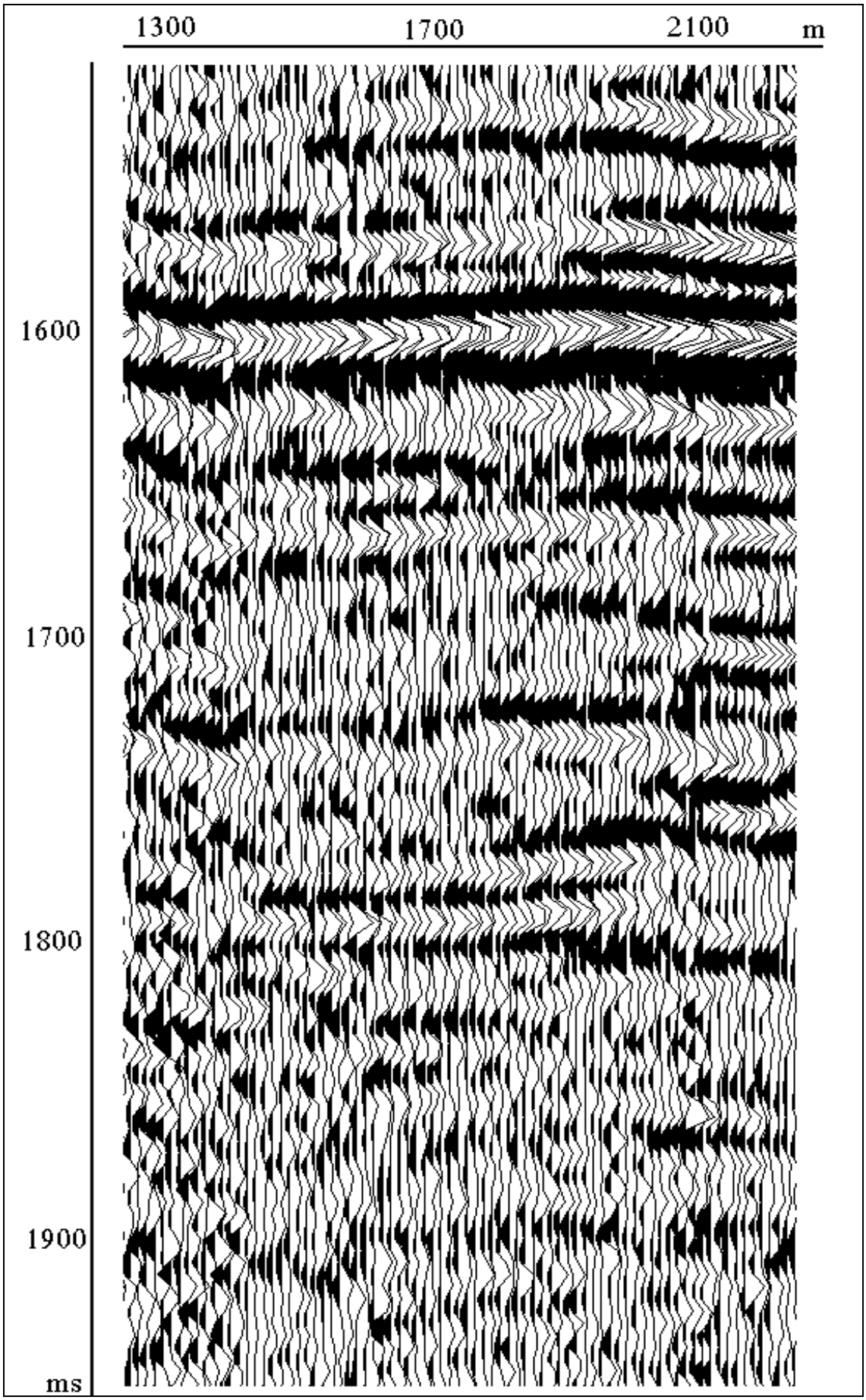

Figure 9(b). Spiking deconvolution.

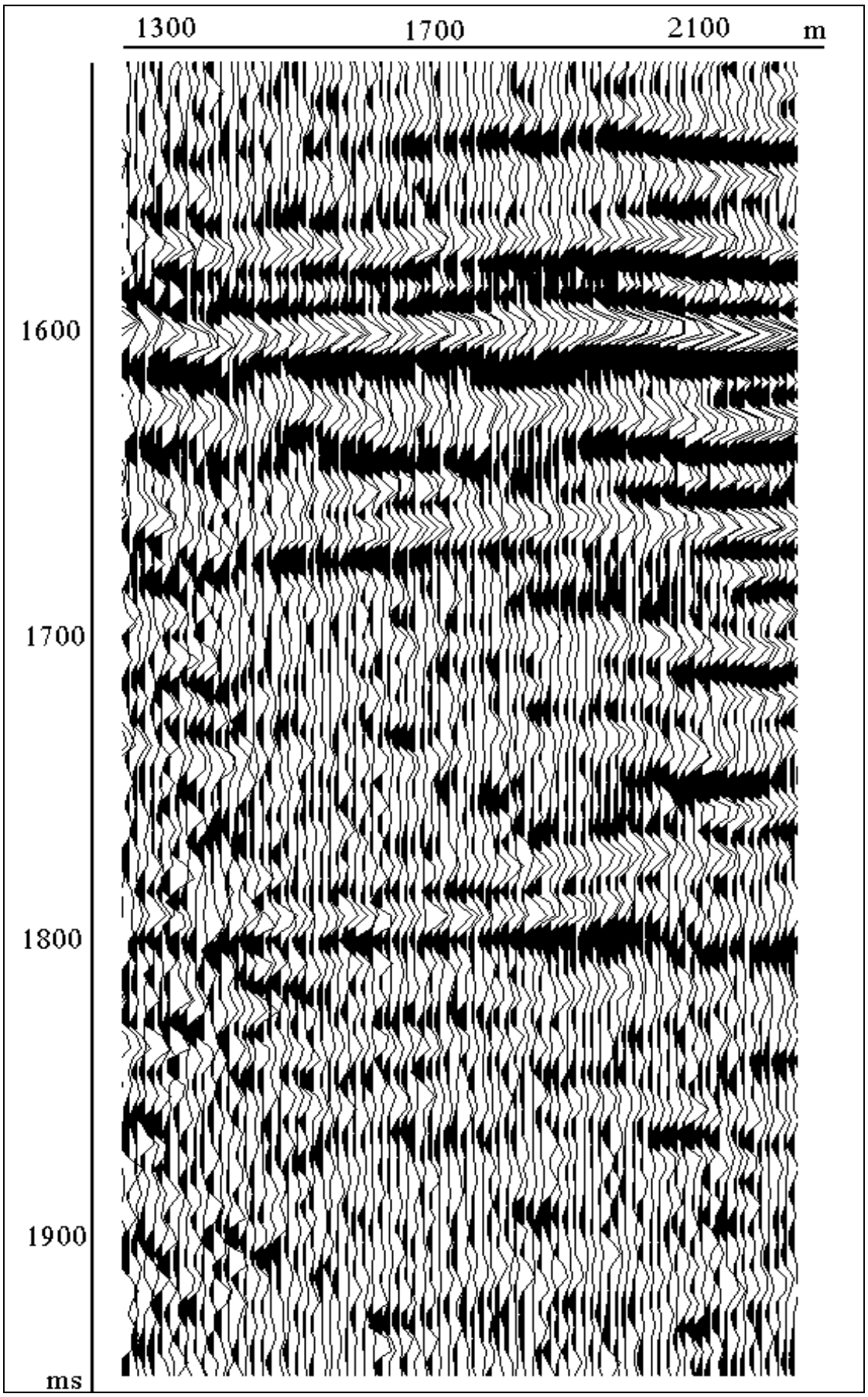

Figure 9(c). Constraint - free amplitude deconvolution.

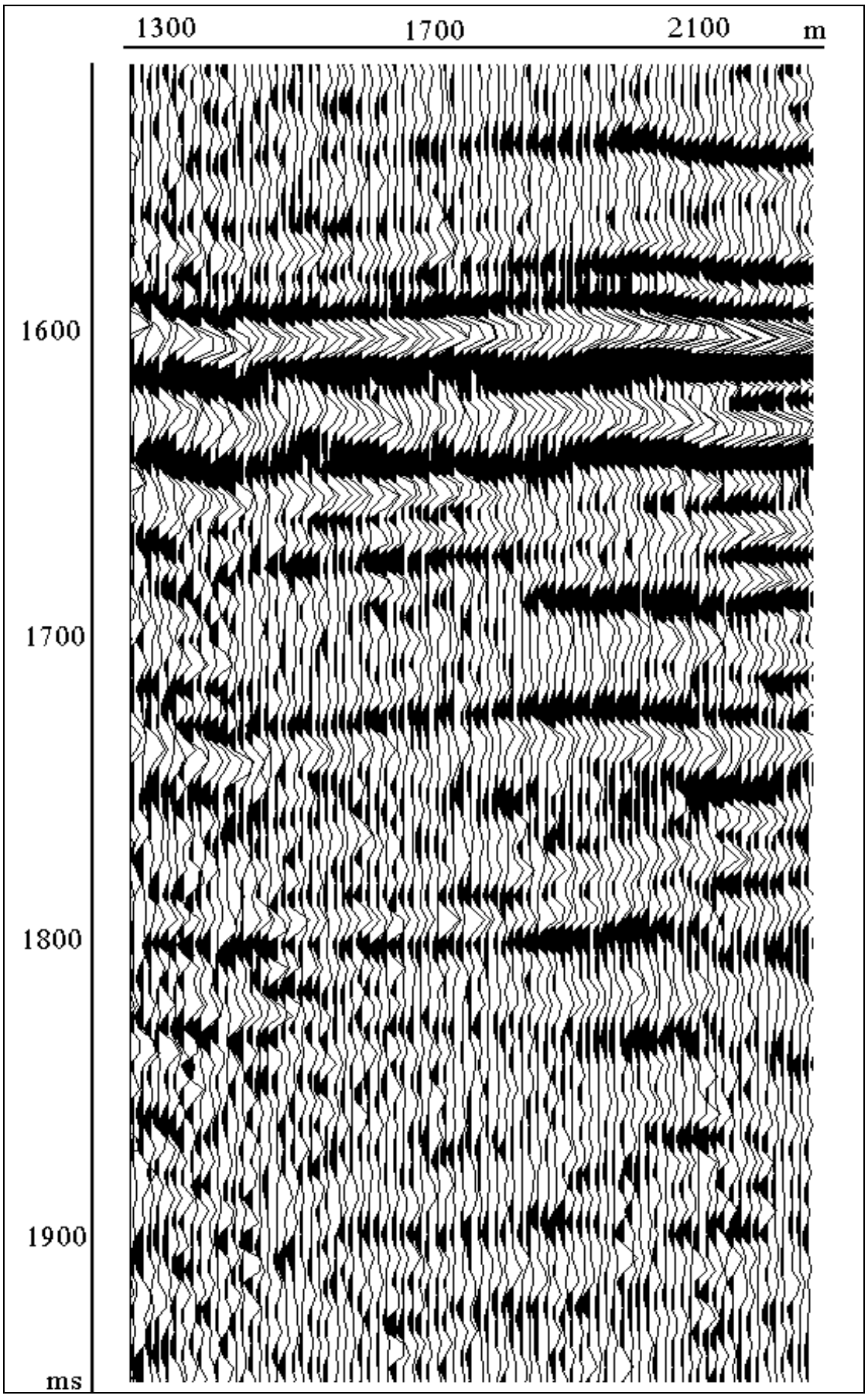

Figure 9(d). Amplitude deconvolution with constraint (8)

The real data processing results are shown in Figure 8, Figure 9. The spectrum estimates given in Figure 7 correspond to these data. It can be easily seen that the wavefield in Figure 8(c),(d) and Figure 9(c),(d) has improved in comparison with the one in Figure 8(b) and Figure 9(b) respectively. The difference among sections in Figure 8(c), Figure 9(c) and Figure 8(d) Figure 9(d) are less significant. But it can be recognised that some events in Figure 8(d) Figure 9(d) show better alignment in comparison with those in Figure8(c) Figure 9(c). Some reflections that have changed significantly are marked by arrows A and B. The event that has arrival at ≈ 1730 ms has changed its appearance.

Certainly these results cannot be considered from the point of view of getting new information about the medium. To do it a more detailed geological interpretation is needed. It can only be claimed that the results obtained can be explained according to the theory presented in this paper.

The results of the tests presented in this paper clearly demonstrate the advantages of the new spectrum estimation method. It is well known that the precision of spectrum estimates plays a key role in deconvolution. Besides, sometimes spectrum estimates are of interest themselves. Since spiking deconvolution is widely used in seismic data processing and the new algorithm utilises its best principles, we hope that this algorithm will be able to replace the methods being applied nowadays.

Figure 5
c) - output,
Figure 9, b) - spiking deconvolution output, c) - a output, d) - output of.